## SEMICONDUCTORS AND DIELECTRICS

# Optical Absorption by $Nd^{3+}$ and $Gd^{3+}$ Ions in Epitaxial Films Grown on $Gd_3Ga_5O_{12}$ Substrates from a Lead-Containing Solution Melt

V. V. Randoshkin\*, N. V. Vasil'eva\*, V. G. Plotnichenko\*\*, Yu. N. Pyrkov\*\*, S. V. Lavrishchev\*\*, M. A. Ivanov\*, A. A. Kiryukhin\*<sup>†</sup>, A. M. Saletskiĭ\*\*\*, and N. N. Sysoev\*\*\*

\* Institute of General Physics, Russian Academy of Sciences, ul. Vavilova 38, Moscow, 119991 Russia \*\* Research Center of Fiber Optics, Institute of General Physics, Russian Academy of Sciences, ul. Vavilova 38, Moscow, 119991 Russia

> \*\*\* Moscow State University, Vorob'evy gory, Moscow, 119992 Russia e-mail: antonv@aha.ru

> > Received July 15, 2003; in final form, November 4, 2003

**Abstract**—Epitaxial films of composition  $(Gd,Nd)_3Ga_5O_{12}$  or  $(Gd,Y,Nd)_3Ga_5O_{12}$  with a neodymium content varying from 0.3 to 15 at. % are grown by liquid-phase epitaxy from a supercooled PbO–B<sub>2</sub>O<sub>3</sub>-based solution melt on  $Gd_3Ga_5O_{12}(111)$  substrates. The optical absorption spectra of the epitaxial films grown are measured in the wavelength range 0.2–1.0  $\mu$ m. The results of interpreting the absorption bands observed in the spectra are used to construct the energy level diagrams of  $Nd^{3+}$  and  $Gd^{3+}$  ions in the matrices of the epitaxial films. © 2004~MAIK~"Nauka/Interperiodica".

#### 1. INTRODUCTION

Neodymium-doped lasers with various solid matrices, especially with those made up of single-crystal garnets (for example, gadolinium gallium garnet Gd<sub>3</sub>Ga<sub>5</sub>O<sub>12</sub>), have been extensively used in quantum electronics [1]. The basic problem of increasing the efficiency of these lasers is associated with the impossibility of growing optically homogeneous crystals with a high concentration of doping rare-earth ions, in particular, Nd<sup>3+</sup> ions, whose distribution coefficient is considerably less than that for the ions replacing them in the matrix [2]. As a result, the concentration of doping rare-earth elements changes significantly along the axis of the growing single crystal.

The above disadvantage can often be eliminated upon changing over to single-crystal films grown by liquid-phase epitaxy from a supercooled solution melt. In this case, the difference between the distribution coefficients of the rare-earth elements introduced into the epitaxial film can be decreased through appropriate choice of the ratio between garnet-forming components in the solution melt. Since only an insignificant amount of these components passes from the solution melt into the film, the concentration of rare-earth elements in the bulk of the film remains almost unchanged over the film thickness.

The first mention of a thin-film single-crystal laser based on an  $Y_{1.25}Ho_{0.1}Er_{0.55}Tm_{0.5}Yb_{0.6}Al_5O_{12}$  garnet film grown on an  $Y_3Al_5O_{12}$  substrate was made in 1972

by van der Ziel *et al.* [3]. In 1973, Bonner [4] succeeded in generating stimulated emission at a wavelength of  $1.06 \, \mu m$  at  $300 \, K$  in  $Y_3 Al_5 O_{12}$  epitaxial films containing 2 at. %  $Nd^{3+}$ .

In this work, we investigated the optical absorption in the wavelength range 0.2–1.0  $\mu m$  in neodymium-containing single-crystal garnet films grown on  $Gd_3Ga_5O_{12}(111)$  substrates through liquid-phase epit-axy from a supercooled PbO–B<sub>2</sub>O<sub>3</sub>-based solution melt.

#### 2. THE GROWTH OF FILMS

Epitaxial single-crystal gallium garnet films with a neodymium content C(Nd) ranging from 0.3 to 15 at. % were grown through liquid-phase epitaxy from a supercooled PbO-B<sub>2</sub>O<sub>3</sub>-based solution melt [5]. For a neodymium content  $C(Nd) \ge 1.7$  at. %, yttrium was introduced into the epitaxial single-crystal films with the aim of matching the lattice parameters of the film and the substrate. The composition of the batch was characterized by the following molar ratios  $(R_1, R_2, R_3)$ :

$$R_1 = [Ga_2O_3]/(\Sigma[Ln_2O_3]) \approx 14.4,$$

$$R_2 = [PbO]/[B_2O_3] \approx 16.0,$$

$$R_3 = (\Sigma[Ln_2O_3] + [Ga_2O_3])/(\Sigma[Ln_2O_3] + [Ga_2O_3] + [PbO] + [B_2O_3]) \approx 0.08,$$

<sup>†</sup> Deceased.

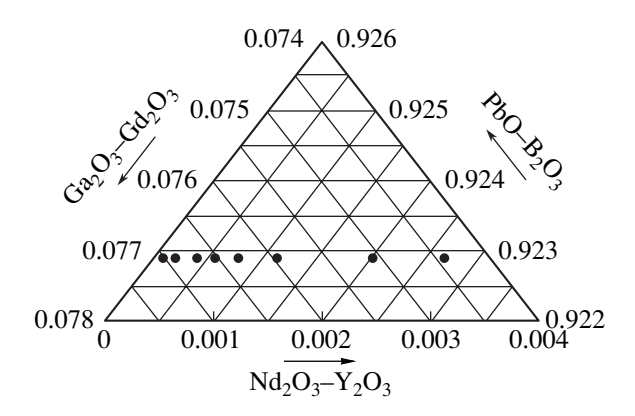


**Fig. 1.** Fragment of the concentration triangle of the  $(Nd_2O_3-Y_2O_3)-(Gd_2O_3-Ga_2O_3)-(PbO-B_2O_3)$  pseudoternary system. Mole fractions of oxides contained in the batch are plotted along the sides of the triangle. Closed circles indicate the compositions of the solution melts used to grow epitaxial single-crystal films of gallium garnets with a neodymium content ranging from 0.3 to 15 at. % (parameters of the films are given in Table 1).

where  $\Sigma[Ln_2O_3] = [Gd_2O_3] + [Nd_2O_3] + [Y_2O_3]$  and brackets designate the oxide content in the batch in mole percent.

The growth experiments are illustrated in Fig. 1, which shows a fragment of the concentration triangle of the ((Nd<sub>2</sub>O<sub>3</sub>–Y<sub>2</sub>O<sub>3</sub>)–(Cd<sub>2</sub>O<sub>3</sub>–Ga<sub>2</sub>O<sub>3</sub>)–(PbO–B<sub>2</sub>O<sub>3</sub>) system. In order to prepare an epitaxial single-crystal film of the specified composition, the ratio between rareearth oxides in the batch was determined with due regard for the known distribution coefficients of the rare-earth elements [2]. Epitaxial films were grown under supercooling conditions ensuring the absence of additional absorption associated with the intervalence pair transitions of Pb<sup>2+</sup> and Pb<sup>4+</sup> impurity ions [6, 7]. The epitaxial single-crystal films thus grown were col-

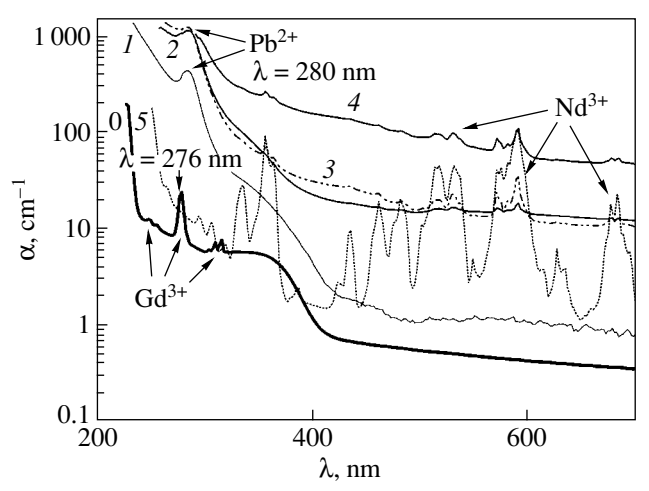


**Fig. 2.** Optical absorption spectra  $\alpha(\lambda)$  for (0) the  $Gd_3Ga_5O_{12}$  substrate; (I) the neodymium-free  $Gd_3Ga_5O_{12}$  film; (2-4)  $Gd_3Ga_5O_{12}$  epitaxial film samples (2) **5**, (3) **7**, and (4) **10** with different neodymium contents; and (5) the  $Nd_3Ga_5O_{12}$  single crystal. The numbering of the films is the same as in Table 1.

orless and optically homogeneous, except the films with a neodymium content  $C(Nd) \approx 15$  at. %, which were yellowish brown and had microcracks.

The solution melt was homogenized in a platinum crucible at a temperature  $T=1100^{\circ}\mathrm{C}$  for 4 h. Then, the temperature was reduced step-by-step to the crystallization temperature of the solution melt. At each temperature step (i.e., at the growth temperature  $T_g = \mathrm{const}$ ), we carried out the growth of the films. As the neodymium content increased, the temperature of saturation  $T_s$  of the solution melt decreased from 1030 to 920°C. The maximum thickness of the epitaxial films grown amounted to 50  $\mu$ m. Thick films with a thickness  $h \ge 25 \mu$ m were grown after an additional homogenization of the solution melt.

**Table 1.** Characteristics of (Gd,Y,Nd)<sub>3</sub>Ga<sub>5</sub>O<sub>12</sub> epitaxial single-crystal films

Sample no.	<i>C</i> (Nd), at. %	$T_g$ , °C	2 <i>h</i> , μm	$f_g$ , µm/min	$\alpha_{806.9},  \text{cm}^{-1}$	Δλ, nm	
1	0.3	999	105.0	0.44	3.8	0.84	
2	0.9	979	76.8	1.28	13.7	0.86	
3	0.9	976	33.4	0.56	16.7	0.87	
4	1.7	950	95.8	0.40	_	_	
5	2.3	964	73.8	0.37	30.6	0.92	
6	3.3	950	53.8	0.90	47.8	0.92	
7	5.0	930	67.9	0.28	76.2	0.92	
8	10.0	944	12.0	0.20	125.0	0.96	
9	10.0	935	68.7	0.19	123.0	0.96	
10	15.0	887	99.8	0.16	176.3	1.01	

Note:  $T_g$  is the growth temperature,  $\alpha_{806.9}$  is the absorption coefficient without regard for scattering at the maximum of the spectral line, and  $\Delta\lambda$  is the half-width of the spectral line at a wavelength of 806.9 nm.

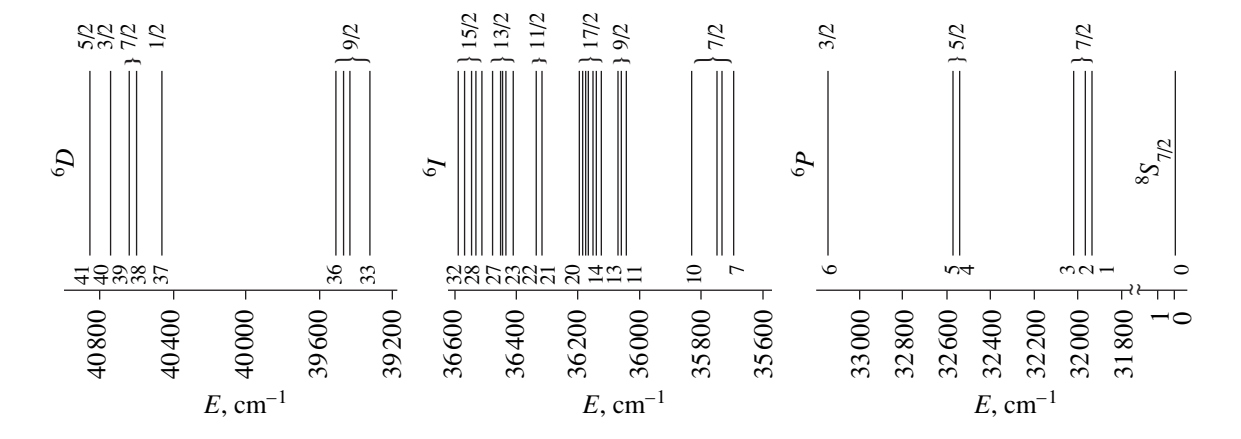
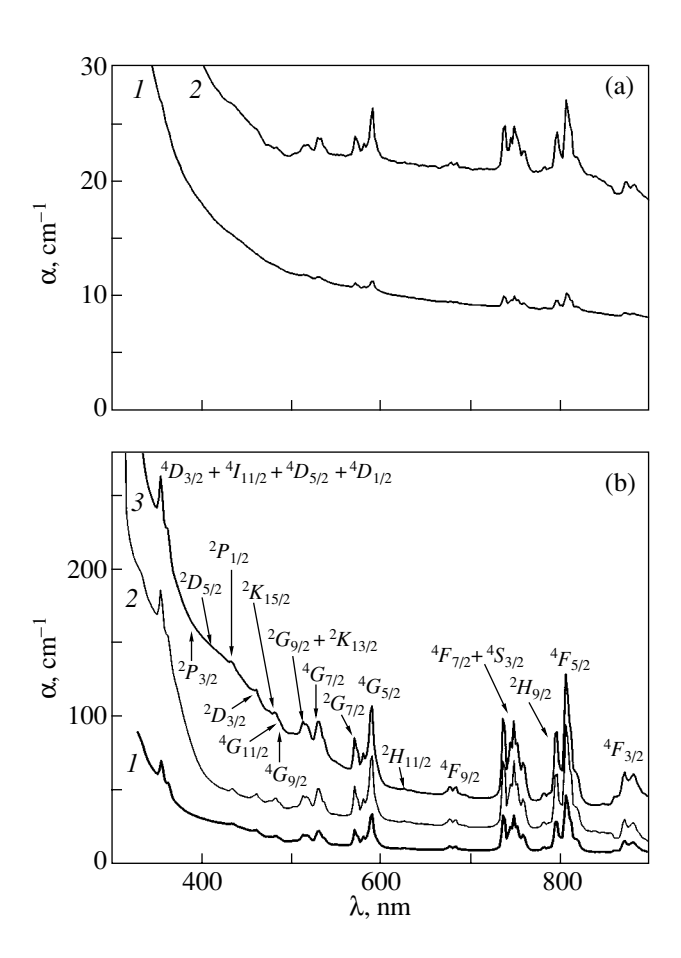


Fig. 3. Diagram of Stark levels of the Gd<sup>3+</sup> ion in the Gd<sub>3</sub>Ga<sub>5</sub>O<sub>12</sub> single crystal at room temperature.

For the above ratio of components in the batch, the growth of films on the surface of the solution melt and platinum auxiliaries was accompanied by spontaneous crystallization of garnet single crystals in the form of tetragonal trioctahedra with {211} facets.



**Fig. 4.** Optical absorption spectra  $\alpha(\lambda)$  for  $Gd_3Ga_5O_{12}$  epitaxial films with different neodymium contents C(Nd): (a) (1) 0.3 and (2) 0.9; and (b) (1) 5, (2) 10, and (3) 15 at. %.

### 3. EXPERIMENTAL TECHNIQUE

The total thickness 2h of the films grown on both sides of the substrate and the growth rate  $f_g$  of these films (Table 1) were determined by weighing the substrate prior to the epitaxial growth and the film–substrate–film structure after the growth. In this case, we ignored the difference in the quantitative compositions of the film and the substrate.

The transmission spectra of the films were measured on a Lambda 900 (Perkin-Elmer) spectrophotometer in the wavelength range  $\lambda=0.2\text{--}1.0~\mu m$  in steps of 2 nm at room temperature.

The absorption spectra of the films were calculated from the transmission spectra as follows. Initially, the transmission spectrum of the substrate, which was measured prior to the growth, was divided by the transmission spectrum of the substrate with the grown films. Then, the natural logarithm of this ratio was divided by the total thickness of the films grown on both sides of the substrate.

#### 4. RESULTS AND DISCUSSION

Figure 2 shows the optical absorption spectra  $\alpha(\lambda)$ for the Gd<sub>3</sub>Ga<sub>5</sub>O<sub>12</sub> substrate (curve 0), the neodymiumfree Gd<sub>3</sub>Ga<sub>5</sub>O<sub>12</sub> epitaxial film (curve 1), Gd<sub>3</sub>Ga<sub>5</sub>O<sub>12</sub> epitaxial films with different neodymium contents (curves 2–4), and the Nd<sub>3</sub>Ga<sub>5</sub>O<sub>12</sub> single crystal (curve 5) grown by the Czochralski technique. As can be seen from Fig. 2, the optical absorption spectra of neodymium-containing films exhibit absorption bands associated with Nd<sup>3+</sup> ions that are characteristic of Nd<sub>3</sub>Ga<sub>5</sub>O<sub>12</sub> single crystals (curve 5). Moreover, these spectra contain an absorption band with a maximum at a wavelength of 280 nm, which, as in the case of Gd<sub>3</sub>Ga<sub>5</sub>O<sub>12</sub> epitaxial films (Fig. 2, curve 1) [6], is attributed to the  $(6s^2)$   ${}^1S_0 \longrightarrow {}^3P_1$  transition of the Pb<sup>2+</sup> ions [8]. It should be noted that all absorption bands of neodymium ions that are characteristic of the

<b>Table 2.</b> Stark levels of the $Gd^{3+}$ ion in the $Gd_3Ga_5O_{12}$ crystal
---

	Nos. of Stark levels	Positions of Stark levels	Number of Stark components				$\Delta E$ ,
Term in the term (Fig. 4)		in the term, cm <sup>-1</sup>	theory	experi- ment	[10] YAG : Gd <sup>3+</sup>	[11] GdCl <sub>3</sub> · 6H <sub>2</sub> O	cm <sup>-1</sup>
$^{8}S_{7/2}$	0	0	4	_	_	_	_
$^{6}P_{7/2}$	1–3	31942, 31972, 32020	4	3	4	4	78
$^{6}P_{5/2}$	4, 5	32545, 32575	3	2	3	3	30
$^{6}P_{3/2}$	6	33150	2	1	2	2	
$^{6}I_{7/2}$	7–10	35694, 35731, 35748, 35834	4	4	4	4	140
$^{6}I_{9/2}$	11–13	36044, 36061, 36071	5	3	5	5	27
$^{6}I_{17/2}$	14–20	36125, 36140, 36150, 36166, 36177, 36184, 36194	7	7	3	7	69
$^{6}I_{11/2}$	21, 22	36320, 36335	6	2	3	5	15
$^{6}I_{13/2}$	23–27	36413, 36438, 36448, 36456, 36482	7	5	_	7	69
$^{6}I_{15/2}$	28–32	36515, 36534, 36549, 36569, 36594	8	5	_	8	79
$^6D_{9/2}$	33–36	39320, 39425, 39464, 39505	5	4	_	5	185
$^{6}D_{1/2}$	37	40465	1	1	_	1	_
$^6D_{7/2}$	38, 39	40602, 40645	4	2	_	2	43
$^{6}D_{3/2}$	40	40748	2	1	_	2	_
$^{6}D_{5/2}$	41	40860	3	1	_	3	_

Nd<sub>3</sub>Ga<sub>5</sub>O<sub>12</sub> single crystal are observed in the absorption spectra of neodymium-containing films.

The optical absorption spectrum of the substrate (Fig. 2, curve 0) exhibits narrow bands in the wavelength range 244-314 nm due to the presence of Gd3+ ions in the substrate. In this range, the transmission spectra were additionally measured in steps of 0.1 nm with a spectral resolution of 0.1 nm. As a result, we revealed 41 maxima in the absorption bands of the spectra. Figure 3 shows the energy level diagram of the Gd<sup>3+</sup> ion in the Gd<sub>3</sub>Ga<sub>5</sub>O<sub>12</sub> single crystal, which was constructed taking into account the data available in the literature [9–11]. Although Hellwege et al. [11] studied GdCl<sub>3</sub> · 6H<sub>2</sub>O and Y(Gd)Cl<sub>3</sub> · 6H<sub>2</sub>O matrices with a nongarnet structure, we used their data for the interpretation of our experimental results. This is explained by the fact that those authors obtained more complete information as compared to Azamatov et al. [10], who investigated the  $Y_{2.95}Gd_{0.05}Al_5O_{12}$  matrix (YAG :  $Gd^{3+}$ ). However, our results of the measurements of the wavelengths at the maxima of the absorption bands proved to be in closer agreement with the data obtained in [10]. Note also that the diagram of the  ${}^6I_{17/2}$  and  ${}^6I_{11/2}$  electron terms obtained in [11] (and, consequently, in our work) differs from that proposed in [10]. The Stark levels shown in Fig. 3 are numerated sequentially starting from the fundamental term  ${}^8S_{7/2}$ . The level positions and complete splittings  $\Delta E$  of the electron terms of the  $Gd^{3+}$  ion in the  $Gd_3Ga_5O_{12}$  single crystal at room temperature are listed in Table 2. Since the ground state of the  $Gd^{3+}$  ion at room temperature corresponds to a single level (level 0 in Fig. 3), the absorption spectrum of the  $Gd_3Ga_5O_{12}$  single crystal contains bands associated with the transitions from the ground state to excited states of the  $Gd^{3+}$  ion.

Moreover, we revealed that the short-wavelength edge of the absorption band of Gd<sup>3+</sup> ions in the Gd<sub>3</sub>Ga<sub>5</sub>O<sub>12</sub> epitaxial films with a neodymium content of 15 at. % is shifted by 0.014 nm toward the longer wavelength range with respect to the absorption band of the Gd<sup>3+</sup> ion in the substrate. In order to determine this shift, we measured the absorption bands associated with the substrate and films in the wavelength range from 270 to 285 nm with a step of 0.2 nm and a spectral resolution of 0.05 nm. This shift can be attributed to the distortion of the crystal lattice at a high neodymium content, which is confirmed by the formation of microcracks in the epitaxial films at C(Nd) = 15 at. %. Therefore, we can state that the energy level diagram of the Gd<sup>3+</sup> ion in the grown films differs from that of the Gd<sup>3+</sup> ion in the Gd<sub>3</sub>Ga<sub>5</sub>O<sub>12</sub> single crystal (Fig. 3) in terms of the magnitude of the aforementioned shift. For epitaxial films with a lower neodymium content, these energy levels coincide with each other.

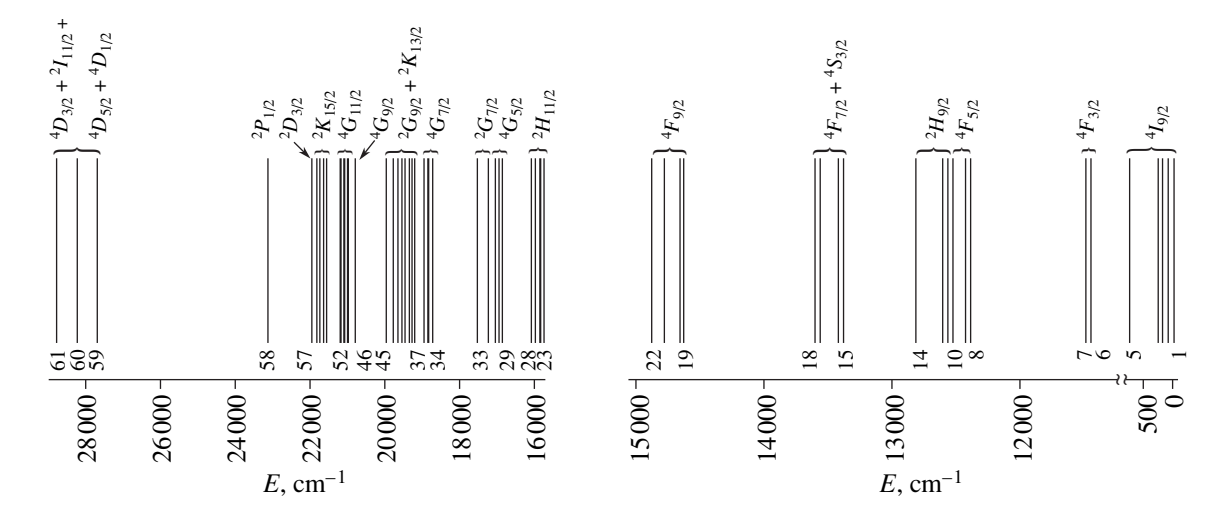
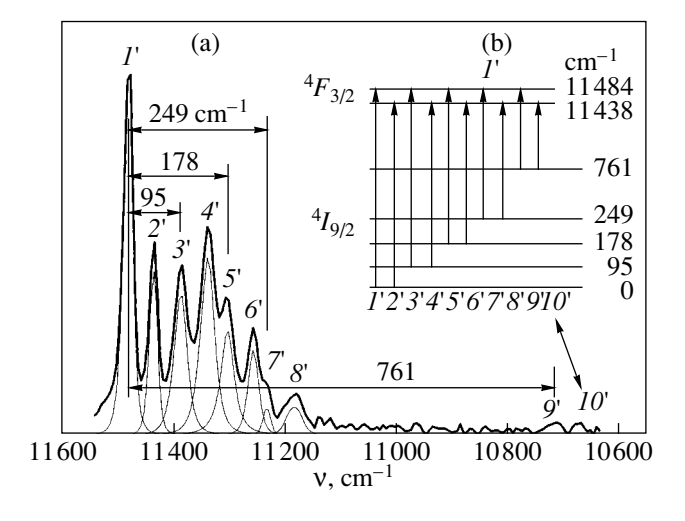


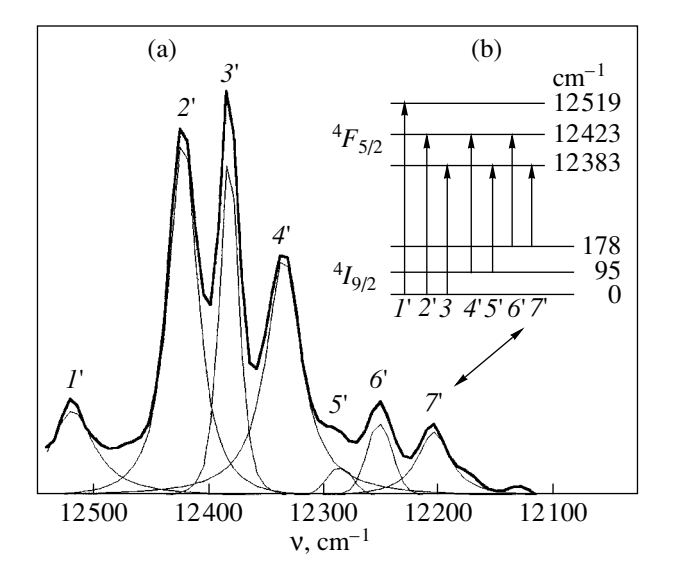
Fig. 5. Diagram of Stark levels of the  $Nd^{3+}$  ion in the  $Gd_3Ga_5O_{12}$ : Nd epitaxial film at room temperature.

Figure 4 shows the absorption bands associated with the presence of neodymium in the epitaxial films and the conventional notation for electron terms of the  $Nd^{3+}$  ion (Fig. 4b) [12, 13]. It turned out that the positions of these bands are independent of the neodymium content and completely coincide with those in the optical absorption spectrum of the  $Nd_3Ga_5O_{12}$  single crystal (Fig. 2). In the general case, both the intensity of each absorption peak and the intensity of absorption at any wavelength in the range under investigation increase in proportion to the neodymium content C(Nd).

The energy level diagram of the  $Nd^{3+}$  ion in the  $Gd_3Ga_5O_{12}$ : Nd film is depicted in Fig. 5. The experimental data on the position of the Stark levels and the complete splitting  $\Delta E$  of the electron terms of the  $Nd^{3+}$  ion in the  $Gd_3Ga_5O_{12}$ : Nd film at a temperature of 300 K are presented in Table 3. In this case, the transmission spectra of the epitaxial films were additionally measured with a step of 0.5 nm and a spectral resolution of 0.5 nm in the wavelength range from 200 to 950 nm. As a result, we revealed 61 maxima of the absorption bands. For the purpose of determining the positions of the Stark levels more exactly, the spectral lines were



**Fig. 6.** (a) Optical absorption spectrum of the  ${}^4I_{9/2} \longrightarrow {}^4F_{3/2}$  transition and the curves of decomposition into components and (b) diagram of the crystalline splitting of the  ${}^4I_{9/2}$  and  ${}^4F_{3/2}$  terms of the Nd<sup>3+</sup> ion in the Gd<sub>3</sub>Ga<sub>5</sub>O<sub>12</sub>: Nd film at room temperature.



**Fig. 7.** (a) Optical absorption spectrum of the  ${}^4I_{9/2} \longrightarrow {}^4F_{5/2}$  transition and the curves of decomposition into components and (b) diagram of the crystalline splitting of the  ${}^4I_{9/2}$  and  ${}^4F_{5/2}$  terms of the Nd<sup>3+</sup> ion in the Gd<sub>3</sub>Ga<sub>5</sub>O<sub>12</sub>: Nd film at room temperature.

**Table 3.** Stark levels of the Nd<sup>3+</sup> ion in the Gd<sub>3</sub>Ga<sub>5</sub>O<sub>12</sub>: Nd film at 300 K

Term	Nos. of Stark levels in the term (Fig. 5)	Positions of Stark levels in the term, cm <sup>-1</sup>	Number of Stark components				$\Delta E$ ,
			theory	experi- ment	[12] Nd : YGaG	[13] Nd : Gd <sub>3</sub> Ga <sub>5</sub> O <sub>2</sub>	cm <sup>-1</sup>
$^{4}I_{9/2}$	1–5	0, 95, 178, 249, 761	5	5	4	5	761
$^{4}F_{3/2}$	6, 7	11438, 11484	2	2	2	2	46
$^4F_{5/2}$	8–10	12383, 12423, 12519	3	3	3	3	136
$^{2}H_{9/2}$	11–14	12565, 12596, 12598, 12810,	5	4	5	5	_
$^4F_{7/2} + ^4S_{3/2}$	15–18	13375, 13415,, 13560, 13597,	6	4	5	6	_
$^4F_{9/2}$	19–22	14638, 14661, 14785, 14884,	5	4	4	4	-
$2H_{11/2}$	23–28	15779, 15840, 15883, 15993, 16088, 16095	6	6	6	6	316
$^4G_{5/2}$	29–31	16888, 16991, 17053	3	3	3	3	165
$^{2}G_{7/2}$	32, 33	, 17266,, 17551	4	2	4	4	_
$^4G_{7/2}$	34–37	18771, 18828, 18872, 18986	4	4	4	4	215
$^{2}G_{9/2} + ^{2}K_{13/2}$	38–45	19248, 19324, 19383, 19494, 19570, 19692, 19821, 19991	12	8	10	10	743
$^4G_{9/2}$	46, 47	,, 20813, 20825	5	2	3	4	-
$^4G_{11/2}$	48–52	21012,, 21089, 21116, 21171, 21190	6	5	5	6	178
$^{2}K_{15/2}$	53–56	21602, 21679,,, 21768, 21867	8	4	6	6	265
$^{2}D_{3/2}$	57	21978	2	1	_	1	-
$^{2}P_{1/2}$	58	23172	1	1	1	1	-
$^{2}D_{5/2}$	_	_	3	-	3	3	-
$^{2}P_{3/2}$	_	_	2	_	2	_	-
${}^{4}D_{3/2} + {}^{2}I_{11/2} + {}^{4}D_{5/2} + {}^{4}D_{1/2}$	59–61	27718*, 28270*, 28854*	12	3	_	_	_

Note: The ellipsis ... indicates the position of the Stark levels, which we failed to determine in the grown films. The level positions marked by an asterisk require further refinement.

decomposed into components with the use of a specially developed program. The results of this decomposition with numbering of the maxima of the absorption bands are presented in Figs. 6a-8a. The diagrams of the crystalline splitting of the electron terms of the Nd<sup>3+</sup> ion in the Gd<sub>3</sub>Ga<sub>5</sub>O<sub>12</sub>: Nd film are depicted in Figs. 6b-8b.

In order to determine the absorption coefficient at the maximum of the absorption band at a wavelength of 806.9 nm (Table 1), we additionally measured the transmission spectra for the films and substrates in the wavelength range from 770 to 860 nm with a step of 0.1 nm and a spectral resolution of 0.1 nm. As the neodymium content increases, the absorption coefficient in the absence of scattering increases from  $3.8 \text{ cm}^{-1}$  at C(Nd) = 0.3 at. % to  $176.3 \text{ cm}^{-1}$  at C(Nd) = 15 at. %. The half-width (the full width at half-maximum) of this band also increases from 0.84 to 1.01 nm, respectively. For calcium niobium gallium garnet

(CNGG) and calcium lithium niobium gallium garnet (CLNGG) crystals doped with neodymium ions at C(Nd) = 1 at. %, the full width at half-maximum is equal to 4 nm. For yttrium aluminum garnet (YAG) crystals with the same neodymium content, the full width at half-maximum is approximately equal to 1 nm. The absorption coefficient at a wavelength of 807.5 nm is equal to 4 cm<sup>-1</sup> for CNGG and CLNGG and 12 cm<sup>-1</sup> for YAG [14].

It should be noted that, during double passage of a semiconductor diode laser at pumping wavelengths of 805 and 808 nm, epitaxial films with a neodymium content C(Nd) = 1.7-3.3 at. % absorb approximately 1/3 of the power. Therefore, these films can be used in crossbeam lasers. Moreover, epitaxial films with a neodymium content up to 3.3 at. %, for which the luminescence lifetime can be as long as 60  $\mu$ s [5], hold promise for lasing.

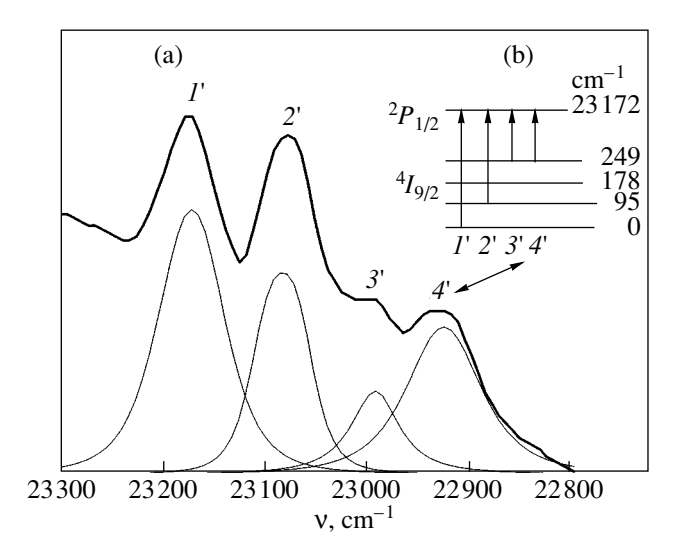


**Fig. 8.** (a) Optical absorption spectrum of the  ${}^4I_{9/2} \longrightarrow {}^4P_{1/2}$  transition and curves of the decomposition into components and (b) diagram of the crystalline splitting of the  ${}^4I_{9/2}$  and  ${}^4P_{1/2}$  terms of the Nd<sup>3+</sup> ion in the Gd<sub>3</sub>Ga<sub>5</sub>O<sub>12</sub>: Nd film at room temperature.

#### 5. CONCLUSIONS

In this work, we obtained the following results.

- (i) Neodymium-containing single-crystal gallium garnet films with a neodymium content varying from 0.3 to 15 at. % were grown by liquid-phase epitaxy from a supercooled PbO– $B_2O_3$ -based solution melt on  $Gd_3Ga_5O_{12}(111)$  substrates.
- (ii) The energy diagram of Stark levels was constructed for different electron terms of the  $Gd^{3+}$  ion in  $Gd_3Ga_5O_{12}$  at room temperature.
- (iii) It was found that the short-wavelength edge of the absorption band of Gd<sup>3+</sup> ions in epitaxial films at a neodymium content of 15 at. % is shifted by 0.014 nm with respect to that in the substrate.
- (iv) The positions of the Stark levels of the Nd<sup>3+</sup> ion were determined for (Gd,Nd)<sub>3</sub>Ga<sub>5</sub>O<sub>12</sub> and (Gd,Y,Nd)<sub>3</sub>Ga<sub>5</sub>O<sub>12</sub> epitaxial films at room temperature.

#### **ACKNOWLEDGMENTS**

We would like to thank M.I. Belovolov, A.V. Vasil'ev, V.F. Lebedev, and S.N. Ushakov for their assistance in performing this work and participation in helpful discussions.

#### REFERENCES

- 1. A Handbook on Lasers, Ed. by A. M. Prokhorov (Sovetskoe Radio, Moscow, 1978), Vol. 1, p. 237.
- V. V. Randoshkin, V. I. Chani, and A. A. Tsvetkova, Pis'ma Zh. Tekh. Fiz. 13 (4), 839 (1987) [Sov. Tech. Phys. Lett. 13, 348 (1987)].
- 3. J. P. van der Ziel, W. A. Bonner, L. Kopf, and L. G. van Uitert, Phys. Lett. A **42A** (1), 105 (1972).
- 4. W. A. Bonner, J. Electron. Mater. 3 (1), 193 (1974).
- V. V. Randoshkin, M. I. Belovolov, N. V. Vasil'eva, K. A. Zykov-Myzin, A. M. Saletskiĭ, N. N. Sysoev, and A. N. Churkin, Kvantovaya Élektron. (Moscow) 31 (9), 799 (2001).
- V. V. Randoshkin, N. V. Vasil'eva, A. V. Vasil'ev, V. G. Plotnichenko, S. V. Lavrishchev, A. M. Saletskiĭ, K. V. Stashun, N. N. Sysoev, and A. N. Churkin, Fiz. Tverd. Tela (St. Petersburg) 43 (9), 1594 (2001) [Phys. Solid State 43, 1659 (2001)].
- V. V. Randoshkin, N. V. Vasil'eva, A. M. Saletskiĭ, K. V. Stashun, N. N. Sysoev, and A. N. Churkin, Fiz. Mysl' Ross., No. 2, 27 (2000).
- 8. G. B. Scott and J. L. Page, J. Appl. Phys. **48** (3), 1342 (1977).
- A. A. Kaminskiĭ, Laser Crystals (Nauka, Moscow, 1975).
- Z. T. Azamatov, P. A. Arsen'ev, and M. V. Chukichev, Opt. Spektrosk. 28 (2), 289 (1970).
- 11. K. H. Hellwege, S. Hufner, and H. Schmidt, Z. Phys. **172** (4), 460 (1963).
- 12. J. A. Koningstein, J. Chem. Phys. 44 (10), 3957 (1966).
- Kh. S. Bagdasarov, G. A. Bogomolova, M. M. Gritsenko, A. A. Kaminskiĭ, A. M. Kevorkov, A. M. Prokhorov, and S. É. Sarkisov, Dokl. Akad. Nauk SSSR 216 (5), 1018 (1974) [Sov. Phys. Dokl. 19, 353 (1974)].
- Yu. K. Voron'ko, N. A. Es'kov, A. S. Podstavkin,
   P. A. Ryabochkina, A. A. Sobol', and S. N. Ushakov,
   Kvantovaya Élektron. (Moscow) 31 (6), 531 (2001).

Translated by N. Korovin